

Model Development of Large-Scale Spacecraft Fires during the Saffire-IV Experiments

John Brooker[1] and Justin Niehaus[2]
NASA Glenn Research Center, Cleveland, OH 44135, USA

An accidental fire can pose dire consequences to crew safety and mission success. The Saffire Project aims to investigate large-scale fire behavior in microgravity in order to aid in the prediction of spacecraft fires. These series of experiments ignite solid materials within the Northrop Grumman Cygnus vehicle after it departs from a resupply mission to the International Space Station. A model of the Cygnus vehicle during the Saffire-IV experiment was developed using the commercial software PyroSim. The cargo arranged during the descent phase was used for the geometry of the model. In the model, cabin air flows into the Saffire payload while heat and combustion species flow out of the Saffire downstream through a standoff to a bed of sensors called the Far Field Diagnostic. The temperature sensors near the Saffire payload were used to determine the heat addition rate at the outlet of Saffire, while the details of the combustion and stoichiometry are used to determine the species flow at the outlet. Gas measurements previously reported for the Saffire-IV experiments are compared against the simulation results and sources of error are discussed.

Nomenclature

A	=	Sample Area
AP	=	Aft Port
AS	=	Aft Starboard
ECLSS	=	Environmental Control and Life Support System
FDS	=	Fire Dynamics Simulator
FP	=	Forward Port
FS	=	Forward Starboard
HAR	=	Heat Addition Rate
ISS	=	International Space Station
MLR	=	Mass Loss Rate
NG	=	Northrop Grumman
NIST	=	National Institute of Standards and Technology
PMMA	=	Polymethyl Methacrylate
SCM	=	Secondary Constant Mass
SCV	=	Secondary Constant Volume
RS	=	Remote Sensor
SFU	=	Saffire Flow Unit
SR	=	Spread Rate
SIBAL	=	Solid Inflammatory Boundary at Low-Speed fabric

I. Introduction

A fire inside of a spacecraft poses a catastrophic threat to crew health and mission success. Most of the fire testing that has been performed to design vehicles and determine material flammability limits has been performed on earth in 1-g or has been small in scale[1,2,3,]. The Saffire project aims to fill knowledge gaps of large-scale flame spread in microgravity. Saffire experiments have also provided opportunities to test novel gas species sensor technology in a realistic flight configuration, as well as a way to obtain data on the length of time to detection and detector signal level for a species release event in a spacecraft cabin. Five Saffire experiments have been conducted so far with one more, Saffire-VI, scheduled to fly in 2023. All will take place on Northrop Grumman's (NG) Cygnus vehicle following the

[1] Aerospace Engineer, Low-Gravity Exploration Technology Branch, 21000 Brookpark Road, Cleveland, OH 44135.
[2] Aerospace Engineer, Low-Gravity Exploration Technology Branch, 21000 Brookpark Road, Cleveland, OH 44135.

completion of its resupply mission to the International Space Station (ISS). The experiments and data downlink take place during the three weeks between undocking from the ISS and burning up during destructive reentry.

The first three Saffire experiments focused on flame spread to compare large-scale microgravity tests to previous small-scale and 1-g tests[4-8]. Saffire IV and V incorporated gas species release events and other diagnostics tools (e.g., far-field trace gas and particle sensors) with the aim of gaining a deeper understanding of smoke plume transport and combustion products on the vehicle.[9,10,11]. Saffire IV has various events that include a CO_2 scrub, flow visualization, gas release and burn events. The burn events include a cotton/fiber-glass blend known as SIBAL and transparent rigid plastic polymethyl methacrylate (PMMA), which is often substituted for glass, such as in shatter proof windows. Far field diagnostics were added for measuring smoke particles and combustion products in order to assess the impact of fire on the vehicle, such as product mixing. Six remote sensors (RS) that measure CO_2 concentration and temperature are also located throughout Cygnus.

It is important to understand the impact a fire has on the vehicle and the crew. The data collected by Saffire will help modelers develop tools to better predict the effect of a fire on a spacecraft. This work aims to develop a model that can predict the burn events in Saffire IV. The model is a closed pressure chamber of the Cygnus vehicle filled with trash and cargo after the resupply mission of NG-13 is completed. In the model, the Saffire unit inputs ambient temperature cabin air and outputs hot air and species to imitate the effect of the combustion events. The heat addition rate (HAR) outputted by Saffire is derived using the difference between the experimentally captured inlet and outlet temperature of Saffire. Downstream of Saffire, near the hatch of Cygnus (zenith) is the Far Field Diagnostic (FFD), where particle and combustion gas sensors are located. The model compares the experimental temperature and CO_2 at the six RS locations throughout Cygnus and the FFD at the opposite end of Cygnus from Saffire.

II. Saffire Experiment

All Saffire experiments have taken place on the NG Cygnus vehicle after a resupply mission to the ISS. The first three Saffire missions focused on the large-scale flame spread in order to determine if tests conducted in 1-g and at smaller scales are relevant to large-scale microgravity flame tests. The next three Saffire tests share that focus, while extending to the smoke plume transport and the fire's effect on the vehicle.

Figure 1 shows a schematic of a Cygnus vehicle with Saffire and the FFD but with the cargo hidden. Cygnus is a pressure vessel that is approximately 4 meters in length by 3 meters in diameter. The Environmental Control and Life Support System (ECLSS) that circulates air throughout the cabin takes air in by the side with the FFD (zenith), and expels it on the side near Saffire, (nadir).

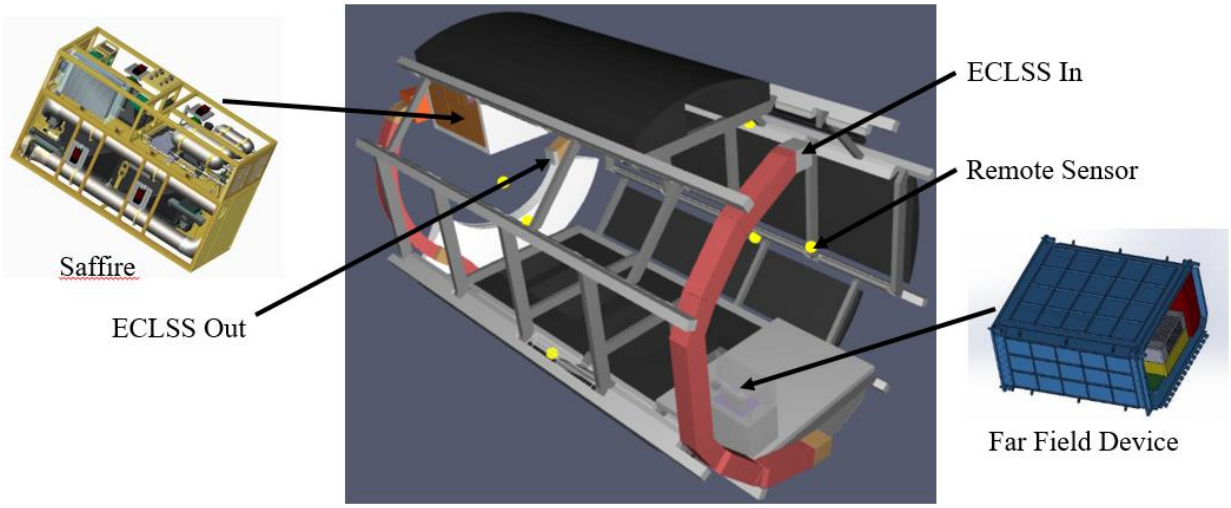

Figure 1. Schematic of Saffire experiment. *The Saffire payload (left) is integrated into the Cygnus vehicle (center). During the experiment, the effect of the fire on the vehicle is determined in part by the Far Field Diagnostic (right).*

The crew maintained a generally prescribed free-air volume in the vehicle, consisting of interconnected channels of approximate triangular geometry, made out of trash and cargo, which transported heat, species and smoke during the campaign events. This produced four triangular stand offs for the transfer of gas from nadir to zenith end cones, and back through the recirculation of air through the ECLSS system.

For context, Table 1 gives all the events completed during Saffire-IV. The test campaign began with a scrub of CO_2 by pulling cabin air through the lithium hydroxide bed of the FFD. In event two, CO_2 was released to determine the volume, which helped determine how much oxygen should be added later in the experiment. Hydrogen Chloride (HCl) was released after the oxygen scrub to study its adsorption to surfaces. HCl was also released during the event 4 SIBAL burn to determine if adsorption changed as a function of temperature. Flow visualization tests were performed before and after the completion of the last burn events to determine if any major differences in air flow through the SFU had occurred. The PMMA in event number 5 did not extinguish when planned, causing the cancelation of other events. More details of the Saffire experiments are provided by Urban[9]. This work focuses specifically on the burn events, test 4 SIBAL burn and the test 5 PMMA burn. Both burns were performed at one atmosphere pressure, 21% O_2 and with concurrent flow relative to the sample through the SFU.

Table 1. Summary of Saffire-IV events. *Events 7 and 8 were not completed due to technical and logistical issues and hence are omitted from this table.*

Event Number	Description of Event	Purpose of Event
1	CO_2 Scrub	Reduce background CO_2, evaluate CO_2 scrubber performance
2	CO_2 and HCl release	Track tracer gas transport throughout cabin for vehicle volume calculation and observe HCl surface adsorption
3	Flow visualization test	Assess SFU air flow
4	Burn: 40.64 cm wide × 50 cm long SIBAL	Sample burn with concurrent HCl release
5	Burn: 40 cm wide × 18 cm long × 1 cm thick 2-sided PMMA	Sample burn, no HCl release
6	CO_2 Scrub	Evaluate CO_2 scrubber performance
9	Flow visualization test	Assess SFU air flow

III. Modeling

Fire Dynamics Simulator (FDS) is a large-eddy turbulent simulation tool developed by NIST for low-speed flow that emphasizes smoke and heat transfer from fires[12]. Pyrosim is the graphical interface that was used to run the simulations of FDS and develop the vehicle model[13]. Figure 2 shows the geometry of the model, highlighting Saffire and sensor locations. The geometry of Cygnus was built from sketches provided by NG. The post resupply cargo and

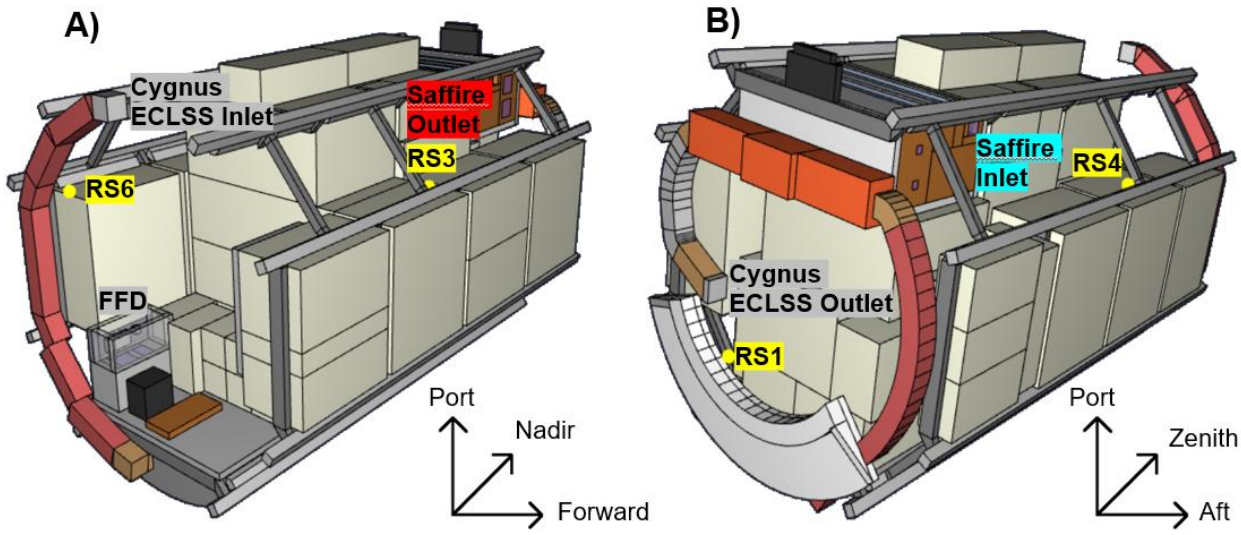

Figure 2. Model of Cygnus vehicle. *A) Shows the outlet of the Saffire unit, where flow moves through the forward port standoff where RS3 is located. RS6 is shown in the far zenith section, along with the FFD. B) The Saffire inlet takes in air from the aft port standoff where RS4 is located. RS1 is shown in the far nadir section.*

trash configuration were determined from crew photos. The free gas volume obtained from the model was 10.9 m^3. This compared favorably with NG's estimate of 11.1 m^3 based on the dimensions of the packed bags.

RS1 is located in the nadir bulkhead section of Cygnus while RS2 is in the forward starboard (FS) standoff. RS3 can be found in the forward port (FP) standoff, which is most directly in the flow path of Saffire. RS4 is in the aft port (AP), RS5 is in the aft starboard (AS), and RS6 is in the far zenith end cone of Cygnus. Figure 2 highlights four of the RS locations in Cygnus, as well as Saffire, the FFD, and the Cygnus ECLSS system that circulates the air. Not shown is RS2, which is approximately in the same location as RS3 but in the FS standoff, and RS5 which is approximately in the same location as RS4 but in the AS standoff.

Table 2 gives flow rates of interest within the model. The flow in the Saffire duct gives a nominal velocity of 20 cm/s, but is ramped down at certain times in the burn. The initial cabin air temperature was set to 25 °C for the SIBAL burn and 26 °C for the PMMA burn, while a constant temperature boundary condition for the surfaces were set at 25 °C for both burns. The heat transfer into the vehicle from Saffire was determined by the experimental Saffire inlet and outlet temperatures. Equation 1 gives the expression for the heat addition rate (HAR) out of Saffire where ρ_{air} is the air density (1.12 kg/m^3), C_p is the isobaric specific heat of the air (1.02 kJ/kg-K), and $\dot{V}_{air}$ is the volumetric flow rate of the air through Saffire, which for the vast majority of the burn is 0.028 m^3/s, as given by Table 2. This method is the sensible enthalpy rise method highlighted by the Society of Fire Protection Engineering Handbook[14]. The specific heat at constant pressure was used due to the vehicle being pressure controlled. The maximum Saffire outlet temperature was 44.9 °C, which gave a ΔT of 15.4 °C for the SIBAL burn and the maximum outlet temperature for the PMMA burn was 87 °C for a ΔT of 57 °C.

Table 2. Model flow rates

Cygnus Location	Flow Rate (m^3/s)
Vehicle	0.062
Saffire Flow Duct	0.028
Saffire Avionics	0.013
FFD	0.017

$$HAR = \rho_{air} C_p \dot{V}_{air} (T_{out} - T_{in}) \quad (1)$$

Figures 3 and 4 give the input parameters for the SIBAL and PMMA burn events respectively. The HAR and SFU flow rate are given on the right axis, and the H_2O and CO_2 generation rates given on the left axis. The flow rate was taken from experimental output and divided into linear segments. The peak generation rate of the products is higher

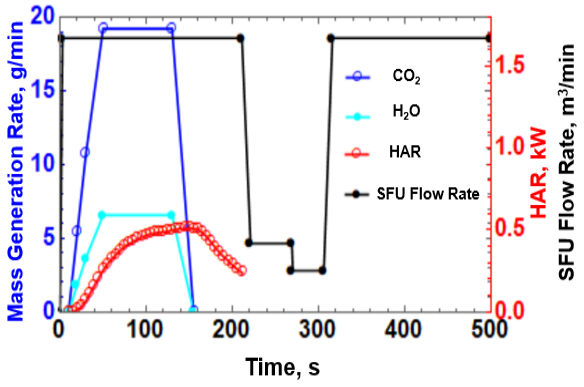

Figure 3. Model inputs for the SIBAL burn event. *The CO_2 and H_2O Mass Generation Rates correspond to the left axis in blue, and the heat release rate coming out of Saffire, as well as the Saffire Flow Rate correspond to the right axis in red and black respectively.*

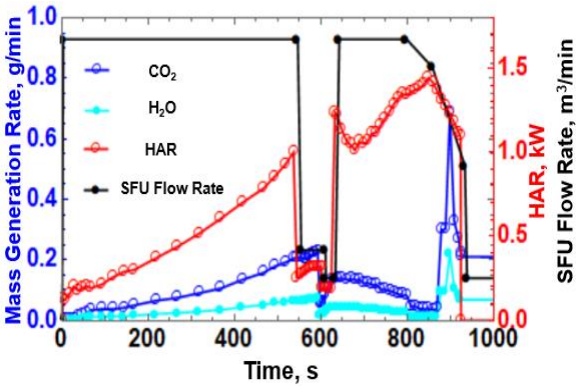

Figure 4. Model inputs for the PMMA burn event. *The CO_2 and H_2O Mass Generation Rates correspond to the left axis in blue, and the heat release rate coming out of Saffire, as well as the Saffire Flow Rate correspond to the right axis in red and black respectively.*

in the SIBAL case, but the burn event is significantly longer in the PMMA event, which generates more overall products. This will be evident in the CO_2 responses shown further in the paper.

The CO_2 and H_2O production rates for the SIBAL burn was determined by assuming stoichiometric combustion and by using the fuel mass loss rate (MLR). This was calculated by the experimental burn rate of the fuel measured in mm/s, as well as the sample area (A) and density (ρ_s) of the sample, as given by Eq. 2. These values are given in Table 3. The stoichiometric equations for cotton and PMMA burning are given by Eq. 3 and 4 respectively, which are used to determine the product yield from the MLR. SIBAL is 75% cotton, which was factored into the calculation.

.

$$\mathrm{MLR}_{cotton} = A\,\rho_S\,SR \tag{2}$$

Table 3. Fuel sample values

	SIBAL	PMMA
Sample Cross Sectional Area (m^2)	1.27×10^{-4}	1.27×10^{-4}
Density (kg/m^3)	573	1180
Max Spread Rate (mm/s)	3.60	-
CO_2 Stoichometric Yield ($kgCO_2/kgFuel$)	1.63	1.76
H_2O Stoichometric Yield ($kgH_2O/kgFuel$)	0.56	0.58

$$C_6H_{10}O_5(\mathrm{v}) + 6O_2 = 6CO_2 + 5H_2O(\mathrm{v}) \tag{3}$$

$$C_5H_8O_2(\mathrm{v}) + 6O_2 = 5CO_2 + 4H_2O(v) \tag{4}$$

IV. Results and Discussion

In Saffire-IV, the temperature and CO_2 concentration of the RS measurements show varying baseline values due to calibration differences[10]. Consequently, all RS and FFD trends presented here are normalized by their pre-ignition baseline, thereby scaling temperatures and concentrations to initial cabin value. One example of non-normalized data is given for context by Figure 5, which shows the RS3 CO_2 and temperature data for the SIBAL burn. The FFD response, shown in Figure 6, gives an excellent prediction. The model captures the upward trend in the FFD better than it does with most RS locations, while also providing a better match of the steady state value. The light blue line in Figure 6 gives the mean CO_2 for the vehicle and it compares well with the data at the FFD. This is an indication the vehicle species concentration is well mixed in the section that contains the FFD. Figure 7 gives the RS responses to CO_2. Overall, there is a decent agreement between experimental and model values, with RS1 providing the best fit. The model rises earlier and over-estimate the steady state CO_2 value. RS3 rose the fastest and had the most overshoot of the steady state value since it was in the direct path of the Saffire outlet, with RS6 showing similar behavior for the same reason. The other four had to rely on mixing and diffusion before elevated CO_2 was recorded. Experimentally, RS2 was by far the slowest to respond and did not even reach steady state, while all other responses reached steady state in at least 400 seconds.

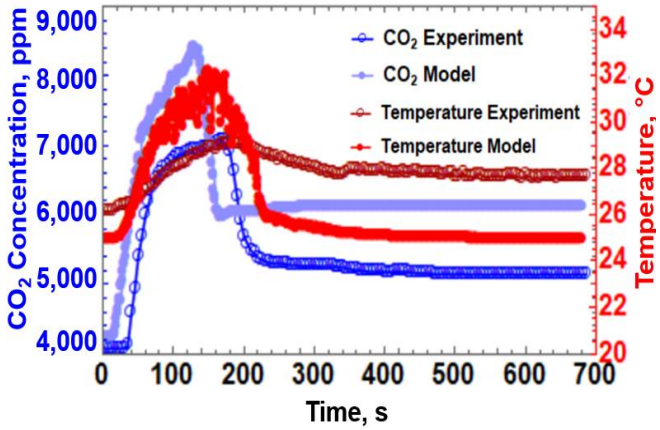

Figure 5. CO_2 and Temperature response from RS3 during SIBAL burn event.

This could be due to a malfunction in the sensor or poor placement within Cygnus, such as being obstructed by too much trash.

Figure 8 gives the temperature at the FFD. A very weak experimental response is shown, while the model response is closest to RS1, RS2, and RS5 that are not directly in the flow path. Also shown in Figure 8 is the mass mean temperature of the model, which analogous to the CO_2 response, compares well with the FFD temperature. Figure 9 gives the RS behavior for the SIBAL burn temperature. Similar to the CO_2 response, the model has a higher temperature response than the experiment. This is most prevalent in RS1, for which the experimental response is slow and does not reach steady state. This could be due to the nadir bulkhead, and other items in that section of Cygnus that absorb heat. This would increase the

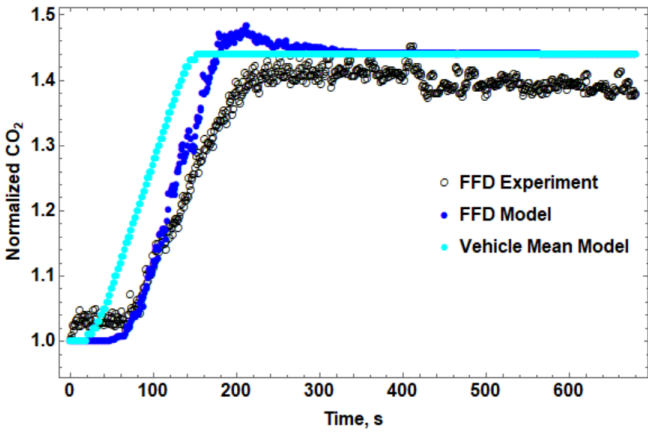

Figure 6. Normalized CO_2 response from FFD and mean vehicle CO_2 concentration during SIBAL burn event.

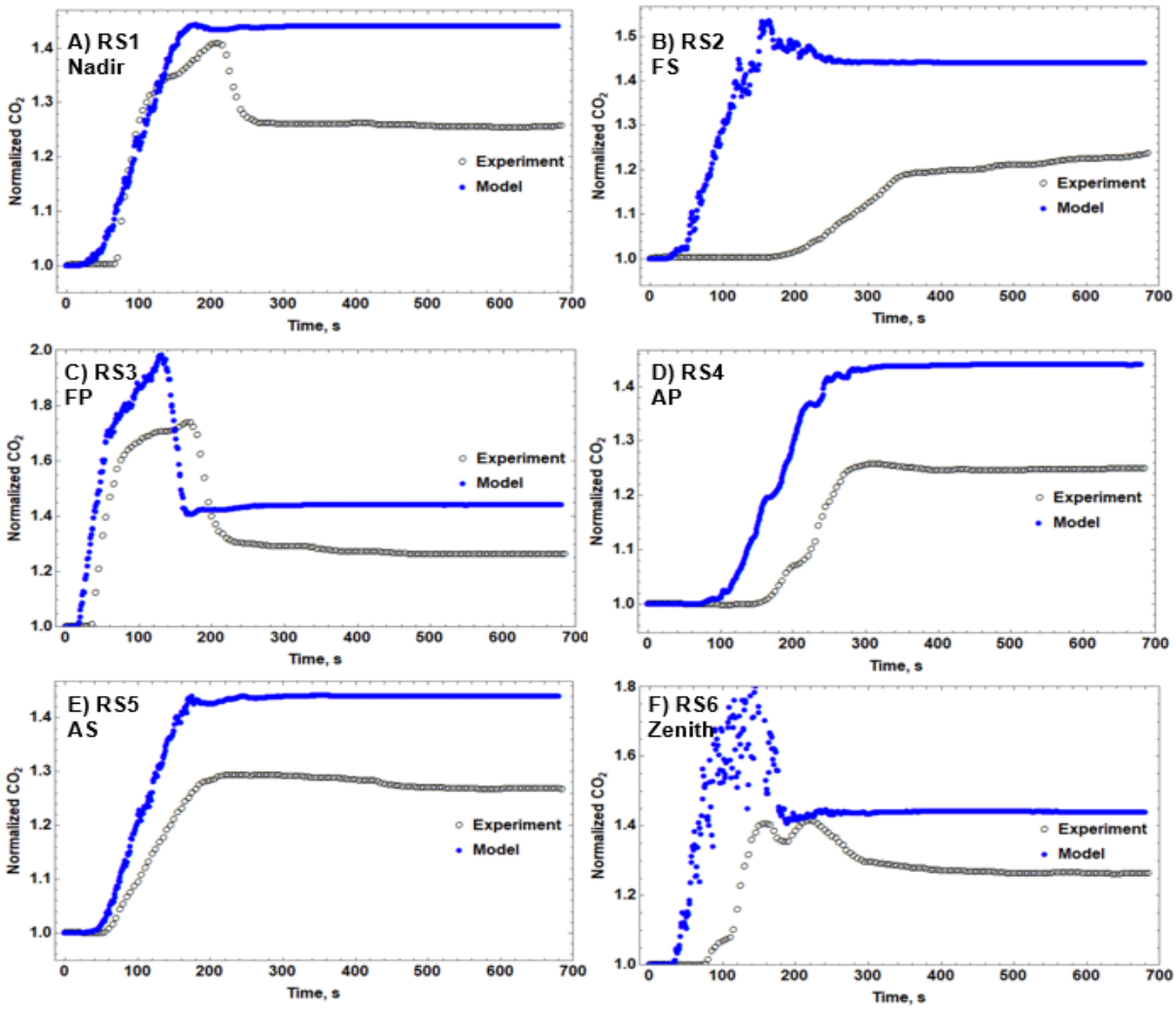

Figure 7. Normalized CO_2 RS responses during SIBAL burn event.

surface temperature of cargo and the spacecraft, decreasing the rate at which heat decreases from the gas phase, as opposed to the constant temperature boundary condition currently use which allows for the maximum heat loss. RS2 seemed unresponsive to the burn event, likely due to the reasons given for the CO_2 response of RS2. As expected, the largest temperature response is given by RS3 and RS6 since they are directly in the flow path, whereas heat response is more a function of mixing and diffusion at the other locations.

A counter intuitive result shows that in many instances, especially for the RS locations in the direct flow path (RS3, RS6), that the data is more noisy in the model results as opposed to the experimental results. There are two possible reasons for this phenomenon. Since the RS uses a

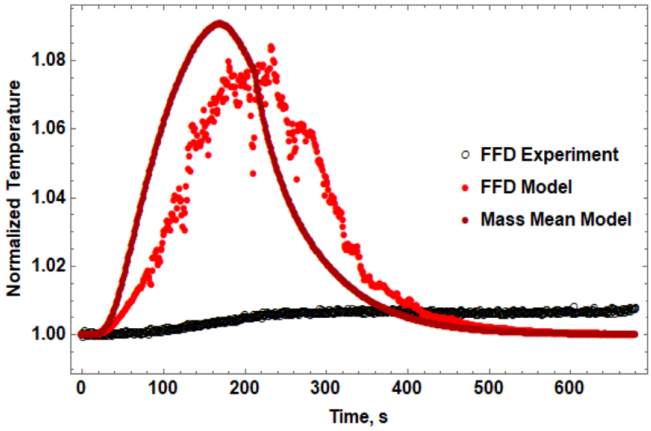

Figure 8. Normalized temperature response from FFD and mass mean vehicle temperature during SIBAL burn event.

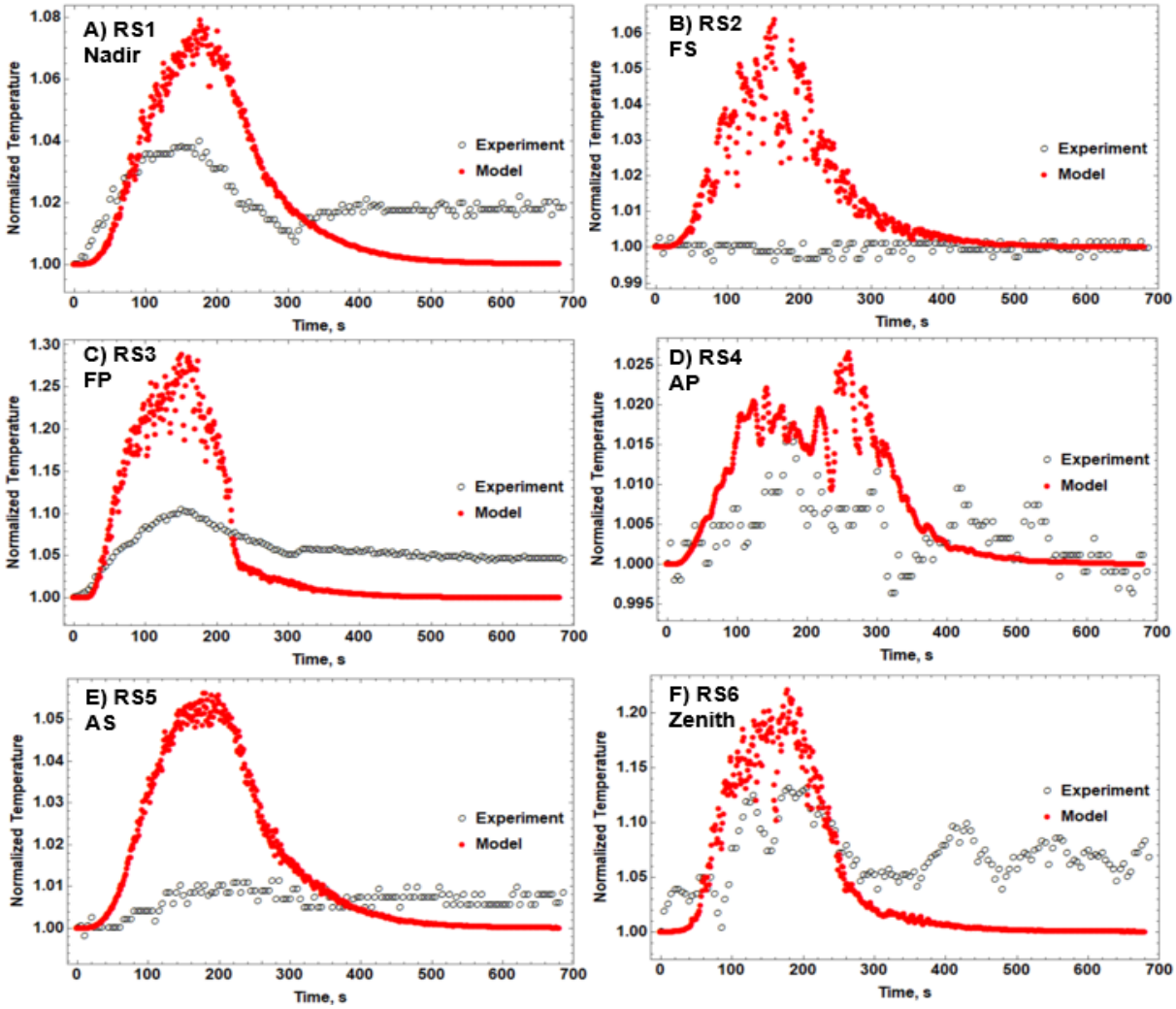

Figure 9. Normalized temperature RS responses during SIBAL burn event.

pump to suck CO_2 at that location to the actual sensor, even if it is a small area, it is averaging concentration around the probe area, which likely smooths out the turbulent effects, whereas in the model, the RS is measuring one node in space and it is directly in the air flow and subject to the turbulent air flow. Another reason for the measured profile being smoother is in the details of how the remote sensors are attached to the beams. While in the model, the beams are just solid rectangular prisms, the real beams resemble I-beams, and have strap hooks to keep the cargo in place. In the experiment, the RS are often behind these strap hooks which also shields it from turbulence.

The PMMA sample was preheated with the igniter at a lower current (1.0 amp for 600 s), and then ignited at 4 amps for 20 s. All charts that

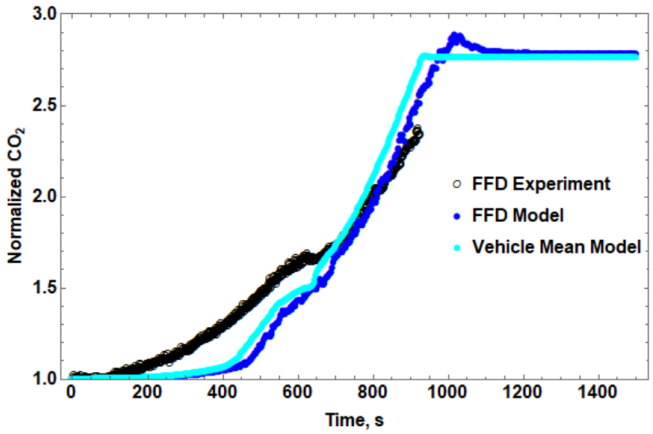

Figure 10. Normalized CO_2 response from FFD during PMMA burn event.

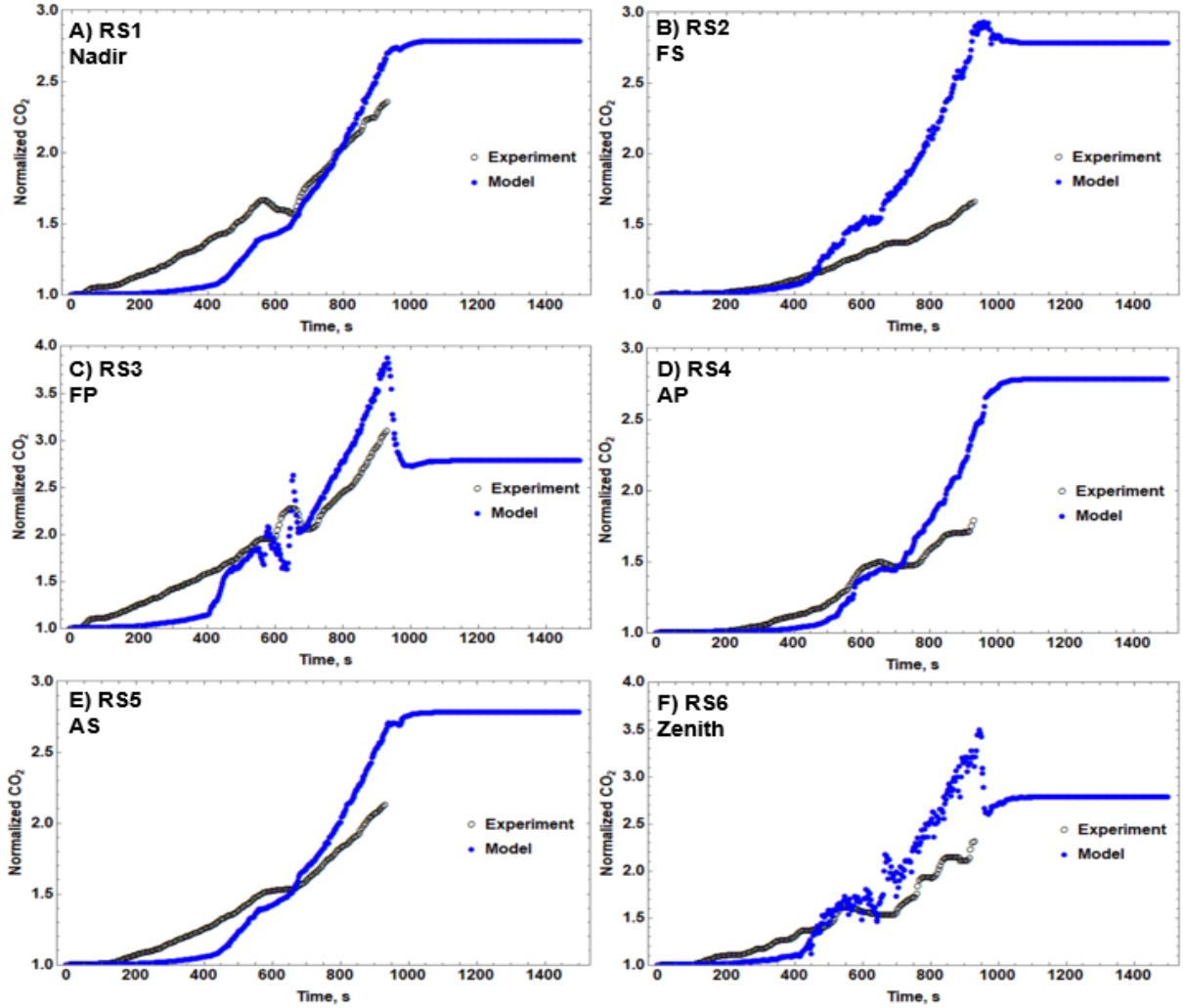

Figure 11. Normalized CO_2 RS responses during PMMA burn event.

include data for the PMMA burn start during the 4-amp ignition phase. This results in a slow increase in CO_2 as the vapor from the preheat is ignited, and rises sharply as the solid begins to be consumed. Unfortunately, the burn was more energetic than expected, causing data to be lost. The data that is there fits well in the increasing phase of the response. Figure 10 gives the FFD CO2 response to the PMMA burn, which provides another good model prediction. As expected, the CO_2 reaches a higher level in the PMMA burn as compared to the SIBAL burn, reaching steady state value that is 2.8 times the baseline value, compared to 1.4 for the SIBAL burn. This corresponds to a steady state CO_2 model value of approximately 11,000 ppm and 6100 ppm for the PMMA and SIBAL event, respectively. Figure

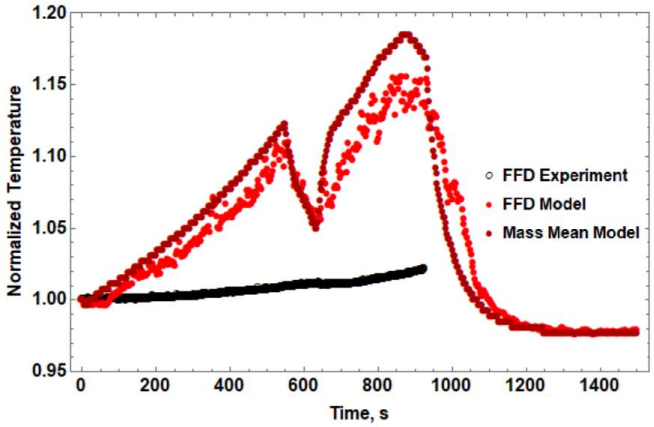

Figure 12. Normalized temperature response from FFD and mass mean vehicle temperature during PMMA burn event.

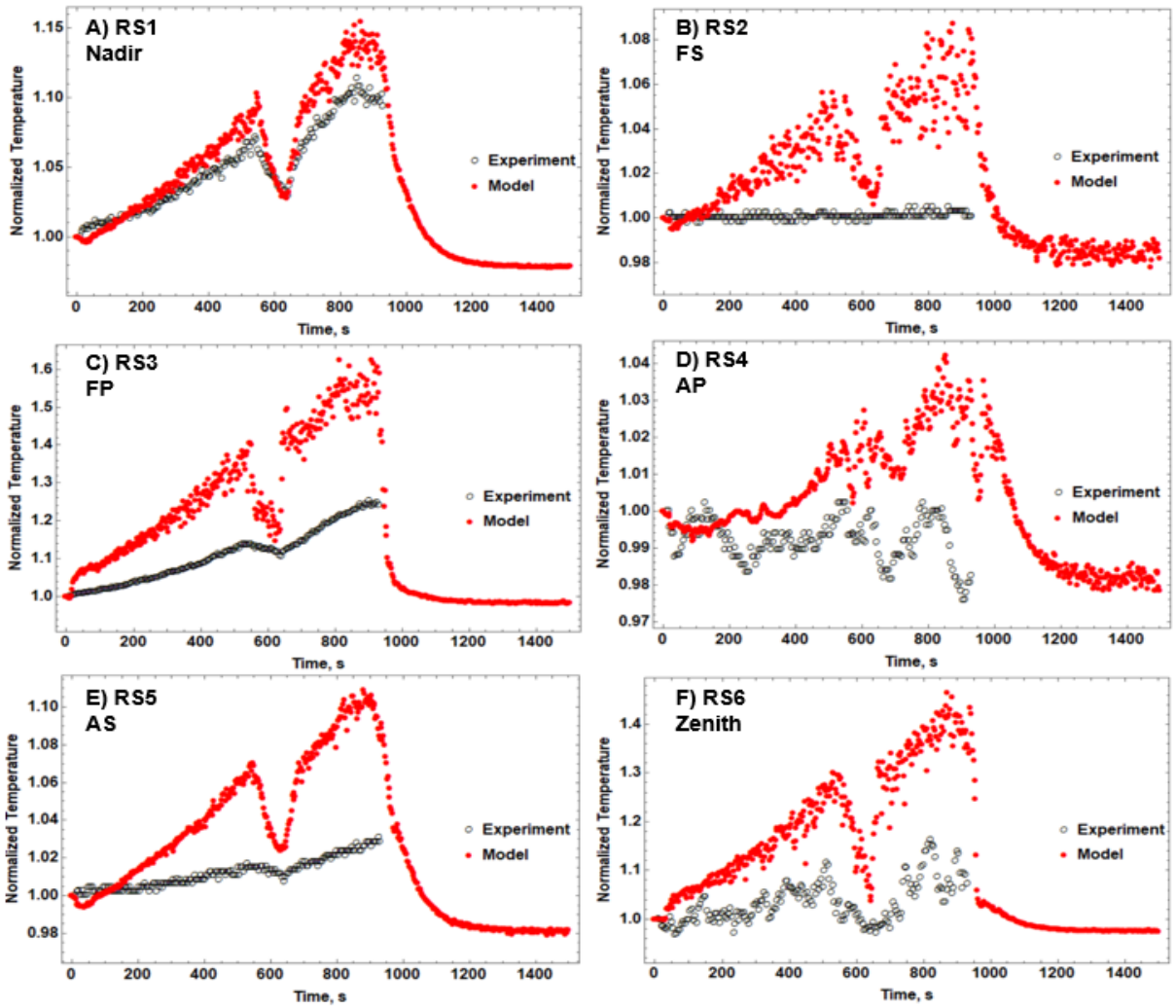

Figure 13. Normalized Temperature RS responses during PMMA burn event.

11 shows the RS CO_2 data for the PMMA burn. Similar to the SIBAL burn, the FFD mirrors RS1, RS4, and RS5 with a steady climb and no overshoot.

Figure 12 gives the FFD temperature data for the PMMA burn. Very similar to the FFD temperature data for SIBAL, there is a very weak response. Figure 13 displays the RS temperature data for the PMMA burn. Being a more energetic fuel, the temperature increases are expectedly higher than the SIBAL burn. The PMMA model seemed to make better predictions of the temperature, especially in the RS1 location. Similar to the SIBAL test, the FFD temperature data shown in Figure 12 was very slow to respond. Since there was good response in other locations where heat and species had to get transported, it is likely that the FFD temperature sensor was surrounded by material that conducted a lot of heat away from the sensor.

In the SIBAL cases, when the SFU fan was turned down around the 200 s mark, the fire was nearly out, and hence no change in the response for the CO_2 or temperature was observed. However, in the PMMA case, turning down the fan did not fully extinguish the fire, and a decrease in CO_2 response can be seen in RS3, RS6 and RS1. While the PMMA flame was put out by the reduced flow, the temperature was still hot enough to vaporize the fuel. Hence, when the fan was turned back on, a deflagration wave ignited the flame again. RS3 and RS6 are in the flow path, therefore changes in Saffire flow will affect those locations disproportionately. RS1 is likely the closest sensor location, so even though it is out of the flow path, there is still some effect. The model predicted a larger dip than was realized by the sensors.

The CO_2 prediction in both burn events over-predicted the steady state CO_2 value. A reason for the difference could be the assumption of stoichiometric combustion. There is a region of the microgravity flame under an oxygen shadow, cast by the upstream part of the flame, which prevents combustion from continuing[9,15]. Soot, CO, unburned hydrocarbons could contribute to the differences between model and experiment. Another reason for the discrepancy is the free volume could be different than what the model and NG predicted. Calculations were performed after the event 2 CO_2 release that predicted a higher free volume[10]. Pressure, temperature, and concentration data from event 2 were used in two independent models, which applied different assumptions to the equations of state. The secondary constant mass (SCM) model divides the total vehicle volume into the free volume, where the released gasses can mix, and a sub-volume of constant mass that does not exchange with the free volume. This model was developed to reflect cargo and trash that approximates sealed volumes where gas cannot escape. Similarly, the secondary constant volume (SCV) model divides the total vehicle volume into two sub-volumes, but instead assumes that the two sub-volumes do exchange gas such that both volumes remain constant. This model can be used to predict gases trapped between bags. In the case of Saffire IV, the SCM and SCV model predicted the same volume of 18.7m^3.

These SCM and SCV models were developed to reflect the potential behavior of trash within Cygnus: the SCM model approximates sealed volumes where gases cannot escape from trash bags, and the SCV model approximates gases trapped between bags. Because these models represent different potential trash packing scenarios, O_2 release conditions are considered based on both models and knowledge of how the vehicle trash was packed. While the model in this work uses perfect rectangular boxes to represent cargo and trash, the real trash bags are amorphous in shape, and the cargo is wrapped in a porous Nomex fabric that could also provide more air for mixing. This increase in volume would explain why the CO_2 in the experiment would reach a smaller steady state value than in the model.

V. Conclusions

A model using NIST's FDS code was developed to determine the effects of the Saffire IV flame events on the Cygnus vehicle. Measurements of CO_2 and temperature were taken at six locations throughout the vehicle, in addition to the FFD. The heat addition rate was calculated based on the inlet and outlet Saffire temperatures, and the product generation rates were calculated based on the flame spread rate and the stoichiometry of combustion of the sample. The model did a reasonable job of predicting the CO_2 data, while over-predicting in some cases. This could be due to a wide range of reasons, with one prevalent reason being the uncertainty in the vehicle free air volume. The model predicted the temperature behavior well on the increasing part of the curve but also over-predicted the peak and decreased faster than the experimental measurement curve. Both the model and the experimental data highlighted the effect a spacecraft fire has on the vehicle, such as product mixing and heat transfer. Better capturing the free volume of the vehicle could provide improvements to the predictive capabilities of the model, as well as changing the surface boundary conditions to allow the participation of surface materials in the adsorption of heat.

Acknowledgments

The Saffire projected was supported by NASA's Advanced Exploration Systems Division. The authors like would like to thank the project manager Gary Ruff and the principal investigator David Urban for their leadership on the project and technical expertise on the subject. Additionally, the authors support the international Saffire science team, with various agencies that include ESA, JAXA, CNES, RSA, DLR, the Russian Academy of Sciences and NASA. The authors are grateful for the efforts of ZIN Technologies, NG, and the on-orbit crew of the ISS on the Saffire project.

References

[1]Fujita, Osamu., "Solid combustion research in microgravity as a basis of fire safety in space," *Proceedings of the Combustion Institute*, Vol. 35.3, 2015, pp. 2487-2502.

[2]Xiaoyang, Z., Liao, Y-T., T., Johnston, M.C., James, S., Ferkul, P., V., and Olson, S., L., "Concurrent flame growth, spread, and quenching over composite fabric samples in low speed purely forced flow in microgravity," *Proceedings of the Combustion Institute* Vol. 36.2, 2017, pp. 2971-2978.

[3]Meyer, M. E., Mulholland, G. W., Bryg, V., Urban, D. L., Yuan, Z.-G., Ruff, G. A., Cleary, T., and Yang, J., "Smoke Characterization and Feasibility of the Moment Method for Spacecraft Fire Detection," *Aerosol Sci. Technol.*, Vol. 49.5, 2015, pp. 299–309.

[4]Ruff, G. A., Urban, D. L., Fernandez-Pello, A. C., T'ien, J. S., Torero, J. L., Legros, G., Eigenbrod, C., Smirnov, N., Fujita, O., Cowlard, A. J., Rouvreau, S., Minster, O., Toth, B., and Jomaas, G., "Spacecraft Fire Experiment (Saffire) Development Status," *44th International Conference on Environmental Systems*, ICES-2014-265, Texas Tech University Libraries, 2014.

[5]Jomaas, G., Torero, J. T., Eigenbrod, C., Niehaus, J., Olson, S. L., Ferkul, P. V., Legros, G., Fernandez-Pello, C., Cowlard, A. J., Rouvreau, S., Smirnov, N., Fujita, O., T'ien, J. S., Ruff, G. A., and Urban, D. L., "Fire Safety in Space – Beyond Flammability Testing of Small Sample," *Acta Astronautica*, Vol. 109, 2015, pp. 208-216.

[6]Ruff, G. and Urban, D., "Operation and Development Status of the Spacecraft Fire Experiments (Saffire)," *46th International Conference on Environmental Systems*, ICES-2016-428, Texas Tech University Libraries, 2016.

[7]Ferkul, P. V., Olson, S., Urban, D. L., Ruff, G. A., Easton, J., T'ien, J. S., Liao, Y.-T. T., Fernandez-Pello, A. C., Torero, J. L., Eigenbrod, C., Legros, G., Smirnov, N., Fujita, O., Rouvreau, S., Toth, B., and Jomaas, G., "Results of Large-Scale Spacecraft Flammability Tests," *47th International Conference on Environmental Systems*, ICES-2017-224, Texas Tech University Libraries, 2017.

[8]Thomsen, M., Fernandez-Pello, A. C., Urban, D. L., Ruff, G. A., and Olson, S. L. "Upward Flame Spread over a Thin Composite Fabric: The Effect of Pressure and Microgravity," *48th International Conference on Environmental Systems*, ICES-2018-231, Texas Tech University Libraries, 2018.

[9]Urban, D., Ruff, G., Ferkul, P., Owens, J., Olson, S., Meyer, M., Fortenberry, C., Brooker, J., Graf, J., Casteel, M., Jomaas, G., Toth, B., Eigenbrod, C., T'Ien, J., Liao, Y.-T., Fernandez-Pello, C., Meyer, F., Legros, G., Guibaud, A., Smirnov, N., and Fujita, O., "Fire Safety Implications of Preliminary Results from Saffire IV and V Experiments on Large Scale Spacecraft Fires," 50th *International Conference on Environmental Systems*, ICES-2021-266, Texas Tech University Libraries, 2021.

[10]Fortenberry, C., Casteel, M., Graf, J., Easton, J., Niehaus, J., Meyer, M., Urban, D., Ruff, G., "Evaluation of Combustion Products from Large-Scale Spacecraft Fires during the Saffire-IV and Saffire-V Experiments," *50th International Conference on Environmental Systems*, ICES-2021-244, Texas Tech University Libraries, 2021.

[11]Wang, X., Zhou, H., Arnott, W.P., Meyer, M.E., Taylor, S., Firouzkouhi, H., Moosmüller, H., Chow, J.C. and Watson, J.G., "Evaluation of gas and particle sensors for detecting spacecraft-relevant fire emissions," *Fire Safety Journal*, Vol. 113, 2020, pp. 102977-102988.

[12]FDS, Fire Dynamics Simulator, Software Package, Ver. FDS6.7.5-0-g71f025606, National Institute of Standards and Technology, Gaithersburg, MD, 2004. http://dx.doi.org/10.6028/NIST.SP.1019.

[13]Pyrosim, Software Package, Ver. 2021-2, Thunderhead Engineering, Manhattan, KS, 2014.

[14]Philip, J., D., *SFPE handbook of fire protection engineering*. 3rd ed., Society of Fire Protection Engineers, Gaithersburg, MD, 2002, Chap. 2.

[15]Prasad, K., Nakamura, Y., Olson, S. L., Fujita, O., Nishizawa, K., Ito, K., & Kashiwagi, T., "Effect of wind velocity on flame spread in microgravity," *Proceedings of the Combustion Institute*, Vol. 29.2, pp. 2553-2560, 2002.